European Journal of Pharmaceutical Sciences 169 (2022) 106090

Contents lists available at ScienceDirect

European Journal of Pharmaceutical Sciences

journal homepage: www.elsevier.com/locate/ejps

Evaluation of the increase of the thymoquinone permeability formulated in polymeric micelles: *In vitro* test and *in vivo* toxicity assessment in Zebrafish embryos

Jessika Lodovichi [a], Elisa Landucci [b], Letizia Pitto [c], Ilaria Gisone [c], Mario D'Ambrosio [d], Cristina Luceri [d], Maria Cristina Salvatici [e], Maria Camilla Bergonzi [a,*]

[a] Department of Chemistry, University of Florence, via U Schiff 6, 50519 Sesto Fiorentino, Florence, Italy
[b] Department of Health Sciences, Section of Clinical Pharmacology and Oncology, University of Florence, Viale Pieraccini 6, 50139, Italy
[c] Institute of Clinical Physiology, National Research Council, Via G. Moruzzi, 1−56124 Pisa, Italy
[d] Department of Neurosciences, Psychology, Drug Research and Child Health (NEUROFARBA), Section of Pharmacology and Toxicology, University of Florence, Viale Pieraccini 6, 50139 Florence, Italy
[e] Institute of Chemistry of Organometallic Compounds (ICCOM)-Electron Microscopy Centre (Ce.M.E.), National Reasearch Council (CNR), Via Madonna del Piano 10, 50019 Sesto Fiorentino, Firenze, Italy

ARTICLE INFO

Keywords:
Thymoquinone
Polymeric micelles
PAMPA
Caco-2 cells
hCMEC/D3 monolayer cells
Zebrafish

ABSTRACT

Thymoquinone (TQ) is a natural compound present in the essential oil and in the fixed oil of *Nigella sativa* L. Like many natural substances, it is characterized by poor aqueous solubility and low stability which limit its bioavailability. Soluplus®-Solutol® HS15 polymeric micelles (TQ-MP) were developed to increase the permeability of TQ with particular attention to overcoming intestinal barrier and the blood brain barrier, for possible oral and parenteral administration. The optimized micelles have dimensions < 100 nm and PdI < 0.2 indicating that the formulation was homogeneous as confirmed also by TEM experiments. EE% was 92.4 ± 0.3%. Stability studies showed a stable formulation following subsequent dilutions and in the gastric-intestinal media.

In vitro studies have revealed that the carrier enhances the permeability of TQ in the intestine and in the blood-brain barrier using Parallel Artificial Membrane Permeability Assay (PAMPA) assay and cellular tests with Caco-2 cells and hCMEC/D3 monolayer cells. Up-take study, cell viability and cytotoxicity studies were also conducted. Fluorescent micelles (FITC-MP), were also optimized to perform *in vitro* up-take study in Caco-2 cells and to study their toxicity in Zebrafish model. The toxicity was evaluated on three lines of Zebrafish: wild type, transgenic line *Tg(Myl7:EGFP)* in which cardiomyocytes are marked with green fluorescence protein and *Tg(flk1-GFP)* line which expresses GFP under the control of the vascular endothelial growth factor receptor 2 (vegfr2) promoter.

1. Introduction

In recent years, natural substances have been widely used in the pharmaceutical, food and cosmetic fields to support or replace the synthetic molecules and they have represented an important source of new compounds, due to the enormous chemical diversity. The reduced toxicity, availability and lower cost of natural constituents compared to many drugs make them an interesting and sustainable alternative for the treatment and prevention of various diseases.

However, their efficacy and clinical application are often limited by poor biopharmaceutical characteristics, including low hydrophilicity, aqueous solubility and intrinsic dissolution rate, and physical/chemical instability. Furthermore, natural substances can have inadequate molecular dimensions with consequent poor absorption, due to the difficulties in crossing biological membranes and therefore poor systemic bioavailability (Bilia et al., 2018).

Thymoquinone (TQ) is the main constituent of the essential oil of *Nigella sativa* L. It is a small molecule from nature with high therapeutic potential (Malik et al., 2021). It is a pharmacologically active substance used as a therapeutic agent as well as for preventive measures (Pal et al., 2021). Interest around this molecule is growing and it is widely investigated from dietary supplementation to chemoprevention and even some clinical trials are ongoing, also as supportive care in patients with COVID-19 (Pal et al., 2021; CTRI/2020/05/025167).

* Corresponding author at: Department of Chemistry, University of Florence, via U. Schiff 6, 50019 Sesto Fiorentino, Florence, Italy
E-mail address: mc.bergonzi@unifi.it (M.C. Bergonzi).

https://doi.org/10.1016/j.ejps.2021.106090
Received 2 September 2021; Received in revised form 18 November 2021; Accepted 18 November 2021
Available online 3 December 2021

Table 1
Physical and chemical properties of empty MP, TQ-MP and Fluorescein isothiocyanate-MP (FITC-MP). Results are expressed as means±SD, $n = 3$ independently prepared batches.

	Size (nm)	PdI	z-potential (mV)	EE%
MP	49 ± 2	0.18 ± 0.02	−3.3 ± 0.4	–
TQ-MP	55 ± 0	0.16 ± 0.01	−8.5 ± 0.8	92.4 ± 0.3
FITC-MP	49 ± 1	0.18 ± 0.00	−8.9 ± 0.3	85.3 ± 4.3

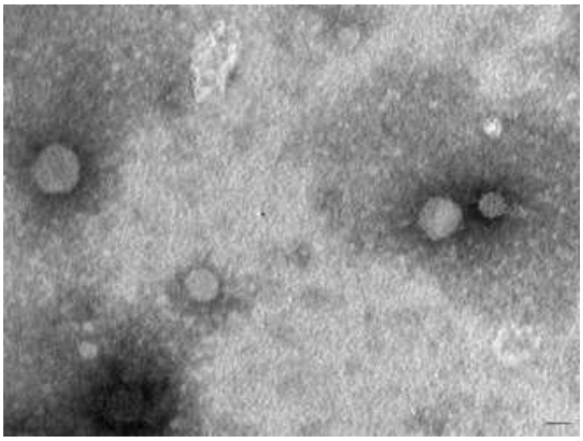

Fig. 1. Transmission Electron Microscope (TEM) images of TQ-MP. Scale bar 50 nm.

TQ has powerful biological antitumor, antioxidant, antimicrobial, immunomodulatory, antihistamine, anti-inflammatory antimicrobial, antiparasitic, anticancer, hypoglycemic, antihypertensive, anti-asthmatic and antirheumatic properties (Banerjee et al., 2010; Darakhshan et al., 2015; Pop et al., 2020; Pal et al., 2021; El-Far et al., 2018; Farkhondeh et al., 2017). There are several studies on its neuroprotective effects, although the mechanism has not yet been fully elucidated. Many studies report the effectiveness of TQ in neurological problems such as epilepsy, Parkinson's, Alzheimer's, anxiety and learning and memory problems. Furthermore, TQ protects brain cells from various injuries thanks to its antioxidant, anti-inflammatory and apoptotic effects (Farkhondeh et al., 2018). In our previously study we showed that TQ have neuroprotective effects in an *in vitro* model of epilepsy that perfectly mimics what occurs *in vivo* models and in humans (Landucci et al., 2021). The results demonstrated that TQ is able to ameliorate the KA-induced increase in unfolded proteins GRP78 and GRP94 expression and it partially rescues the reduction of the KA-induced apoptotic pathway activation; TQ modulates processes leading to neuronal death after exposure to kainate in the CA3 hippocampus area.

Despite the numerous pharmacological activities, TQ has a high instability, rapid elimination and binds for more 99% with plasma proteins, all aspects that limit their clinical use. Its hydrophobicity, poor solubility and bioavailability, sensitivity to light and pH (Salmani et al., 2014), prevent their achievement of the target sites. Its poor aqueous solubility makes it necessary to administer doses much higher than effective oral ones to carry out its activity (Khan et al., 2017).

To date, thanks to the development of nanotechnologies, drug delivery systems have been designed to improve the bioavailability and stability of natural substances. Furthermore, these systems have numerous other advantages such as improving solubility, achieving a gradual and prolonged release over time, enhancing pharmacological activity and intracellular up-take. Nanoformulations of TQ ameliorate the pharmacological potentials of TQ via enhancement of its bioavailability with significant decreases in its required doses. Oral phospholipidic nanomatrix, topical ethosomes and liposomal chitosan gel were developed to improve the stability and oral bioavailability of TQ, enhancing its therapeutic efficacy in a carrageenan-induced paw inflammation model (Rathore et al., 2019; Kausar et al., 2019; Mostafa et al., 2018).

Table 2
Physical and chemical stability of TQ-MP in simulated gastrointestinal fluids. Results are expressed as means±SD, $n = 3$ independently prepared batches.

	Size (nm)	PdI	EE (%)
TQ-MP	56 ± 0	0.17 ± 0.01	92.4 ± 0.3
TQ-MP in SGF	57 ± 2	0.17 ± 0.01	80.1 ± 3.9
TQ-MP in SIF	72 ± 6	0.22 ± 0.01	62.9 ± 0.4

Nanocarrier formulations and surface-modified nanocarriers such as nanoparticles, nanoemulsions, phytosomes, cubosomes, niosomes, liposomes, SNEDDS were developed to improve anticancer and anti-inflammation activities of TQ (Rathore et al., 2020; Ballout et al., 2018; El-Far et al., 2020).

Soluplus®-Solutol® HS15 polymeric micelles of TQ have been shown to enhance the TQ anti-migration activity and to inhibit human SH-SY5Y neuroblastoma cell migration (Bergonzi et al., 2020). The present project is aimed at deepening the influence of micellar formulation on the permeability of TQ, with particular attention to overcoming intestinal barrier and the blood brain barrier, for possible oral and parenteral administration.

The polymeric micelles are an easy-to-prepare delivery system for active molecules, with a high loading capacity of the drug, and can be functionalized on the surface allowing to have an active targeting towards details areas of the body or obtain long-circulating systems.

Empty (MP) and TQ-loaded (TQ-MP) Soluplus®-Solutol® HS15 micelles were prepared with the hydration method of the lipid (Bergonzi et al., 2020) and physically and chemically characterized. A morphological analysis with a transmission electron microscope (TEM) was also performed.

The stability of the formulation in gastric and intestinal media and to dilution were also tested. The influence of carrier on the permeability of TQ was evaluated using Parallel Artificial Membrane Permeability Assay (PAMPA) assay (Kansy et al., 1998; Di et al., 2003; Bergonzi et al., 2014; Graverini et al., 2017; Piazzini et al., 2018, 2019) and cellular tests with Caco-2 cells and hCMEC/D3 monolayer cells as *in vitro* models of intestinal barrier and blood brain barrier, respectively. Up-take study, cell viability and cytotoxicity studies were also conducted. Fluorescent Soluplus®-Solutol® HS15 micelles (FITC-MP), were also developed and characterized to perform *in vitro* up-take study in Caco-2 cells and to track their toxicity in Zebrafish model. The chemical-physical stability of fluorescent formulation was monitored over 10 days, and the *in vitro* release study of the probe from the micelles was performed.

Zebrafish is a very significant *in vivo* model that allows an effective and rapid evaluation of the biodistribution and biosafety of molecules. Zebrafish is a small fish with a genome and physiology of various organs and barriers analogous to those of humans. Important aspect is the transparency that allows imaging of the probes and the distribution of compounds in real time. Zebrafish is widely used for gene studies, drug discovery and toxicological studies.

Indeed, a zebrafish is a significant *in vivo* model for effective and rapid evaluation of whole-body toxicity of nanomaterials (D'Amora et al., 2018; Cassano et al., 2019). Toxicological profiles of different nanomaterials, including metal, silica and polymeric nanoparticles, liposomes, quantum dots, carbon nanotubes, etc., in zebrafish have been reported (Jia et al., 2019; Haque and Ward, 2018; Weber et al., 2014; Van Pomeren et al., 2017; Zhou et al., 2016; Azhari et al., 2021; Rabanel et al., 2020; Li et al., 2017a; Tao et al., 2020; Calienni et al., 2018).

Zebrafish has been considered as a cost-effective, rapid, and high-fidelity method suitable also for therapeutic assessment, biodistribution tracking and a dynamic model to study the transport of nanosized drug delivery systems across the biological barriers (Li et al.,

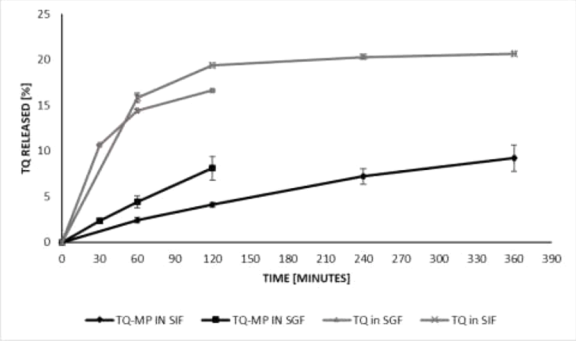

Fig. 2. *In vitro* release profiles in SGF and SIF of TQ from aqueous saturated solution (TQ) and from polymeric micelles (TQ-MP). Results are expressed as means±SD, $n = 3$ independently prepared batches.

2017b; Sieber et al., 2019, 2017c; Azhari et al., 2021; Sieber et al., 2019)

Recently, the interest in this model has grown, as it has proved to be very versatile for the study of the transport of nanomaterials and the biodistribution even of drug delivery systems and to evaluate the sustained release of drugs from nanoformulations (Chakraborty et al., 2009; Kalaiarasi et al., 2016; Weber et al., 2014; Fako and Furgeson, 2009; MacRae and Peterson, 2015; Cassano et al., 2019; Wu et al., 2019).

In this study, Zebrafish was used as an *in vivo* model to assess the morbidity and mortality of drug delivery. The toxicity of TQ-MP was evaluated on three lines of Zebrafish: Wild type (AB), transgenic line *Tg (Myl7:EGFP)* in which cardiomyocytes are marked with green fluorescence protein and *Tg(flk1-GFP)* line which expresses GFP under the control of the vascular endothelial growth factor receptor 2 (vegfr2) promoter.

2. Materials and methods

2.1. Chemicals and reagents

Soluplus® and Solutol® HS15 were provided by BASF (Badische Anilin- und Soda Fabrik, Ludwigshafen, Germany) with the support of BASF Italia and BTC Chemical Distribution Unit (Cesano Maderno, Monza, and Brianza, Italy). Thymoquinone, Phosphate buffered saline BioPerformance Certified pH 7.4 (PBS), Tween 80, Cholesterol BioReagent (≥ 99%), Fluorescein isothiocyanate (FITC, purity ≥ 90%, HPLC), Fluorescein sodium salt (NaF), Sodium chloride (NaCl ≥99,8%), Lipase from porcine pancreas, Pepsin from porcine gastric mucose, Pancreatin from porcine pancreas, Bile salts, Sodium Hydroxide (NaOH ≥98%), Calcium chloride (CaCl2 ≥96%), Hydrochloric acid (HCl ≥37%) were purchased from Sigma Aldrich (Milan, Italy). Porcine polar brain lipid was obtained from Avanti Polar Lipids, Inc., Alabaster, AL, USA. All the solvents used (Methanol, Acetonitrile, Dimethyl sulfoxide (DMSO), Formic acid, Dichloromethane (CH_2Cl_2), Dodecane (≥99%), Ethanol (≈96%)) were HPLC grade from Sigma Aldrich, Milan, Italy. Water was purified by Millipore, Milford, MA, USA, Milli-Qplus system. The 96-well Multi-Screen PAMPA filter plates (pore size 0,45 μm) were purchased from Millipore Corporation (Tullagreen, Carrigtwohill, County Cork, Ireland). Dialysis kit was from Spectrum Laboratories, Inc. (Breda, The Netherlands). Phosphotungstic acid (PTA) was from Electron Microscopy Sciences, Hatfield, PA, USA.

2.2. Preparation of blank mixed micelles (MP)

Blank mixed micelles (MP) were prepared according to the thin film hydration method (Bergonzi et al., 2020). Soluplus® (100 mg) and Solutol® HS15 (400 mg) were dissolved in 10 mL CH_3OH/CH_2Cl_2 mixture (1:4 v/v) and then, solvents were evaporated under vacuum for 20 min at 30 °C. Then, the lipid film was hydrated with 5 mL of deionized water and sonicated for 5 min. The obtained MP were stored at 4 °C.

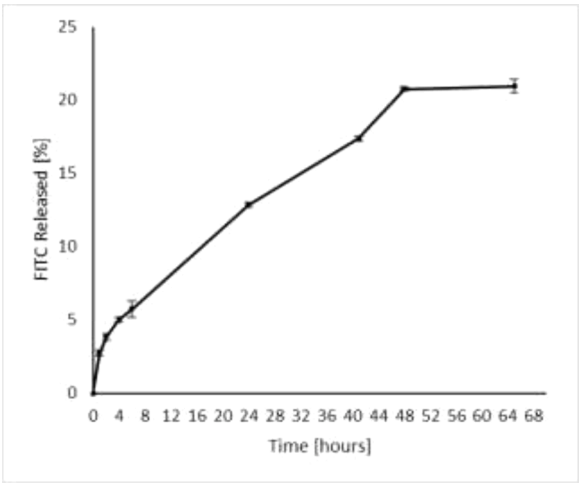

Fig. 3. *In vitro* release profile of FITC from polymeric micelles (FITC-MP). Results are expressed as means±SD, $n = 3$ independently prepared batches.

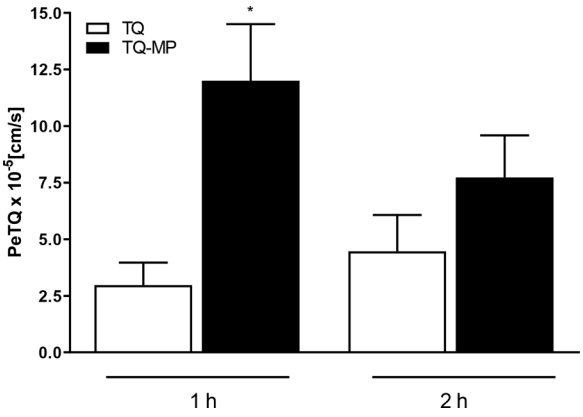

Fig. 4. Pe values of TQ-MP respect to TQ saturated aqueous solution in PAMPA-gastric test. Data are expressed as mean±SD, $n = 3$ independently prepared batches.

2.3. Preparation of TQ-Loaded MP and FITC-Loaded MP

The TQ-loaded MP (TQ-MP) and the fluorescent MP (FITC-MP) were prepared according to the method previously described. TQ or Fluorescein isothiocyanate (FITC) ($\lambda_{ex} = 492$ nm, $\lambda_{em} = 518$ nm, green) were added to lipid phase to obtain a final concentration of 5 mg/mL for TQ and 1 mg/mL for FITC. The formulations were stored at 4 °C, away from light.

2.4. Physical and morphological characterization

The evaluation of the particle size and the polydispersity index (PdI) was performed by dynamic light scattering (DLS) using a Zsizer Nanoseries ZS90 (Malvern Instrument, Worcestershire, UK) at 25 °C. The z-potential was defined using Electrophoretic Light Scattering technique (ELS) employing the same instrument. To avoid multiple scatterings of the light, for all measurements, samples were diluted (1:10 v/v) with deionized water. As reported in Bhattacharjee et al., the pH affects the zeta potential value. The pH of the diluted micellar dispersion resulted 5.45 (Bhattacharjee, 2016). The analyses were performed in triplicate.

The shape and the surface structure of mixed micelles were

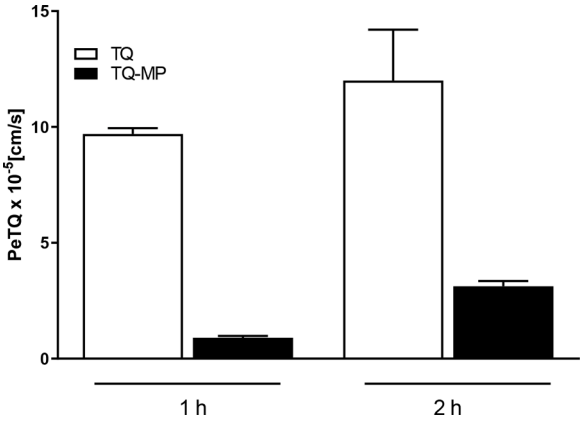

Fig. 5. Pe values of TQ-MP respect to TQ saturated aqueous solution in PAMPA-brain test. Data are expressed as mean±SD, $n = 3$ independently prepared batches.

investigated by transmission electron microscope (TEM, Philips CM12, FEI, USA). The samples were diluted with deionized water (1:5 v/v), then were dropped on a 200 mesh carbon film-covered copper grid and negatively stained with phosphotungstic acid aqueous solution (1% w/v). After drying, the sample was observed with the TEM.

2.5. Determination of encapsulation efficiency

The encapsulation efficiency (EE%) of TQ-MP was determined by membrane filtration method (Hou et al., 2016). The formulation was filtered with a 0.20 μm filter membrane with the aim to retain free TQ. The filtrate was diluted with MeOH (1:20 v/v).

The amount of TQ encapsulated into polymeric micelles was quantified by HPLC (Bergonzi et al., 2020). For the calibration curve, different concentrations ranging from 0.001 μg/mL to 0.1 μg/μL were used.

The EE% of FITC-MP was determined by dialysis bag method. The bag was inserted for 1 h in 1 L of deionized water. Then, the sample was diluted (1:50 v/v) with methanol and sonicated in an ultrasonic bath for 30 min to extract FITC. The solution was centrifuged for 10 min at 14,000 rpm and analyzed by HPLC (Piazzini et al., 2018). The eluents were: (A) formic acid/water pH 3.2; and (B) acetonitrile. The flow rate was set at 0.8 mL/min. The gradient applied was: 0.10 min 90% B, 5 min 60% B, 10 min 50% B, 12 min 45% B, 15 min 45% B, 18 min 10% B and 20 min 90% B. The chromatograms were registered at a wavelength of 224 nm. The calibration curve was prepared using standard FITC, dissolved in methanol from a concentration range of 0.002–0.098 μg/μL.

The EE%, for both methods, was calculated by the following equation:

$$EE\% = \frac{\text{Weight of TQ in micelles}}{\text{Weight of TQ fed}} \times 100$$

2.6. Stability studies

2.6.1. Storage stability study

Dialyzed FITC-MP were stored as dispersion at 4 °C. The stability was monitored for 10 days by DLS and HPLC analyses monitoring the particle size, PdI, z-potential and EE%

2.6.2. Stability studies afterwards subsequent dilutions

The TQ-MP were diluted (1:10, 1:50, 1:100, 1:300 and 1:500 v/v) with deionized water. Then, the physical properties of the formulation were checked by DLS analyses.

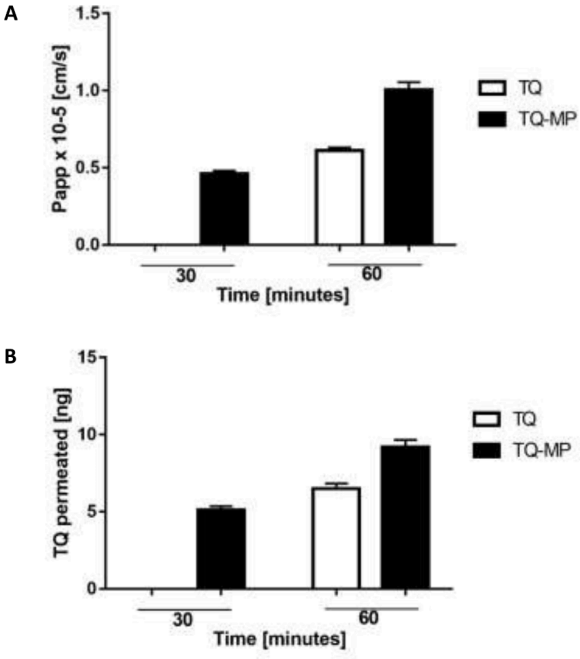

Fig. 6. A: Caco-2 apparent permeability (Papp) of free TQ and TQ-MP. B: Amount of free TQ and TQ-MP permeated across Caco-2 cells layer. Data are expressed as mean±SEM, $n = 3$ independently prepared batches.

2.6.3. Stability in simulated gastrointestinal conditions

The TQ-MP was incubated in simulated gastric fluid (SGF) for 2 h at 37 °C under magnetic stirring at 250 rpm and subsequently in simulated intestinal fluid (SIF) for further 6 h at 37 °C under magnetic stirring at 250 rpm. SGF was obtained dissolving 2 g of sodium chloride, 3.2 g of pepsin and 7 mL of HCl in 1 L of deionized water. The pH of the solution was adjusted to 1.2. The composition of SIF was: lipase (4,8 mg/mL), bile salts (5 mg/mL), pancreatin (0.5 mg/mL) and calcium chloride 750 mM in 1 L of deionized water. The pH was adjusted to 7.0. The effect of SGF and SIF on physical and chemical properties of TQ-MP were evaluated by measuring particle size, PdI and EE%.

2.7. In vitro release studies

2.7.1. TQ release in simulated gastrointestinal conditions

TQ release from MP was studied by the dialysis bag method. Two mL of TQ-MP or TQ saturated solution were added to a regenerated cellulose dialysis membrane (Spectrum Laboratories, Inc., Breda, The Netherlands, MWCO 12–14 kD) and then immersed in 200 mL of the release media at 37 °C under magnetic stirring. The release media was SGF or SIF. TQ release was monitored for 2 h in SGF, and 6 h in SIF. At predetermined intervals, 1 mL of release medium was taken for HPLC analyses and replaced with the same volume of release media (Piazzini et al., 2019). All experiments were performed in triplicate.

2.7.2. FITC release

FITC release from MP was developed according to the method previously described. The release medium was a solution of PBS and Tween 80 (0.5% w/v) and the release was monitored during 24 h. At predetermined intervals, 1 mL of release medium was collected for HPLC analyses and replaced with the same volume of release media. All experiments were performed in triplicate.

2.8. PAMPA experiments

PAMPA was carried out on 96-well filter plates (Millipore, Billerica, MA, USA).

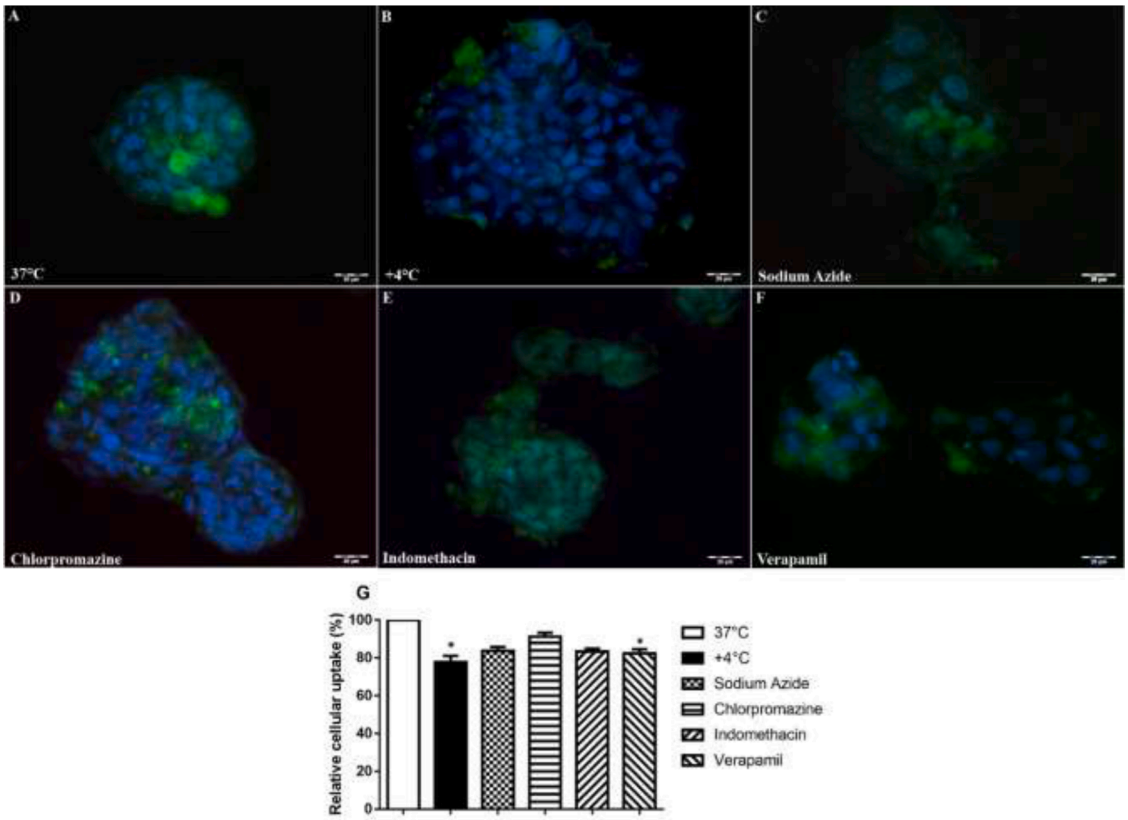

Fig. 7. Densitometric analysis of cellular uptake of FITC-MP. Results are expressed as mean±SEM, $n = 5$. *$p < 0.05$ vs 37 °C by Kruskal-Wallis test and Dunn's multiple comparisons test. Scale bar 20 μm.

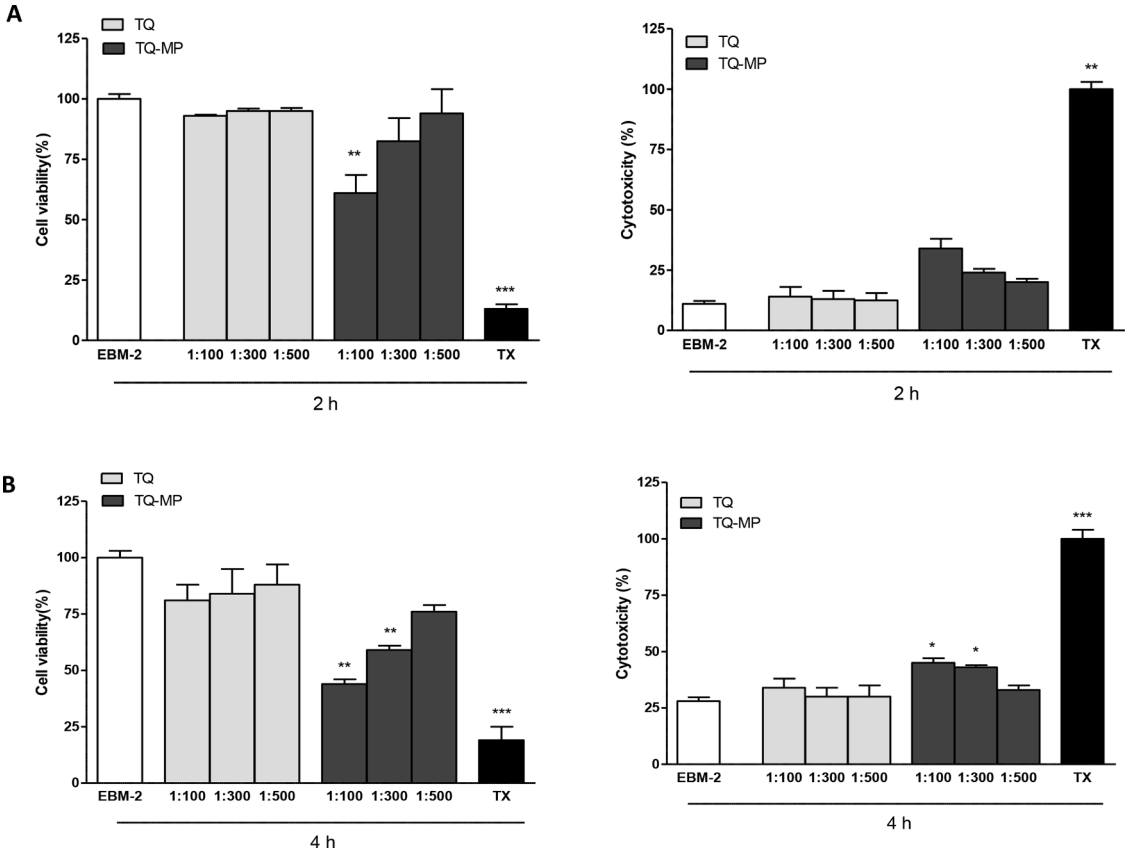

Fig. 8. A: hCMEC/D3 cell viability evaluated by cytotoxicity by LDH assay (left panel) and MTT assay (right panel) when exposed for 2 h to TQ or TQ-MP. Data are expressed as percentage of control (EBM-2 medium) and Triton-X which represent, respectively, the maximum cell viability and cell cytotoxicity. B: hCMEC/D3 cell viability evaluated by cytotoxicity by LDH assay (left panel) and MTT assay (right panel) when exposed for 4 h to TQ or TQ-MP. Values represent the mean ± SEM of at least three experiments performed in triplicate. *$p < 0.05$, **$p < 0.01$, ***$p < 0.001$ vs. EBM-2 alone.

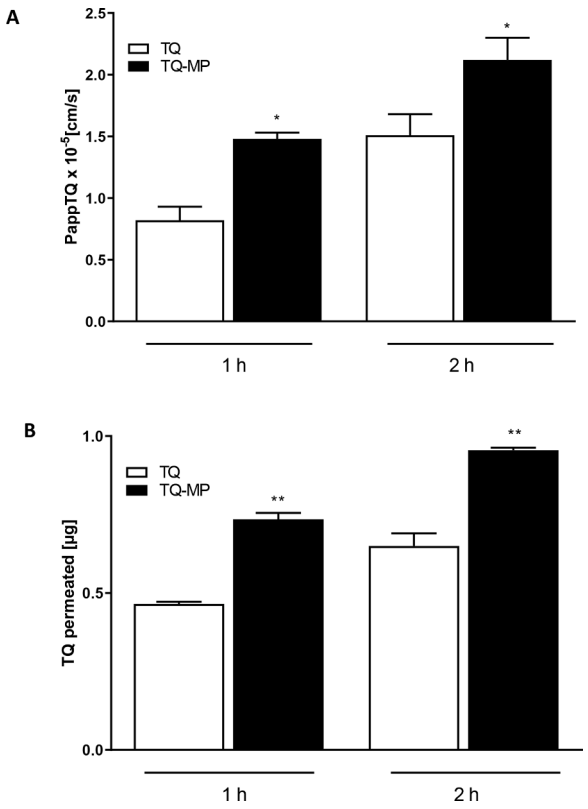

Fig. 9. A: hCMEC/D3 cells apparent permeability (P_{app}) of free TQ and TQ-MP. Data are expressed as mean±SD, $n = 3$. B: Amount of free TQ and TQ-MP permeated across hCMEC/D3 cells layer. Data are expressed as mean±SD, $n = 3$.

2.8.1. PAMPA gastric

The acceptor plate was filled with 250 µL of PBS/EtOH solution (7/3 v/v) and the 96-well microliter PVDF filter plate was impregnated with 10 µL of a lecithin (1% w/v) and cholesterol (0,8% w/v) in 1,7-octadiene solution. The donor plate was filled with 250 µL of TQ-MP or TQ in DMSO/EtOH solution. The plate assembly was placed into a sealed container to prevent evaporation and incubated at room temperature for 2 h. After the incubation, the samples of the donor and acceptor compartment were diluted with methanol (1:50 v/v) and TQ concentration was determined by HPLC. The assay was performed in triplicate. The effective permeability (P_e, cm/s) was estimated with the following equation:

$$P_e = \frac{-\ln\left(1 - \frac{Ca}{Cep}\right)}{A\left(\frac{1}{Vd} + \frac{1}{Va}\right)t} \text{ where } C_{eq} = \frac{(Cd\ x\ Vd) + (Ca\ x\ Va)}{Va + Vd}$$

A is the active surface area, Vd and Va the well volume of the donor and acceptor plate, respectively, t the incubation time (s), Ca and Cd the concentration of TQ in the acceptor and donor plate at time t, respectively.

2.8.2. PAMPA brain

The procedure was the same as above but each artificial membrane was derivatized with 5 µL of Porcine Polar Brain Lipid (PBL 2% w/v) and cholesterol (1% w/v) in n-dodecane solution. Right after the activation of the artificial membrane, 250 µL of TQ-MP or free TQ solution were added to each donor compartment (Piazzini et al., 2018).

2.9. Caco-2 cell culture experiments

2.9.1. Cell lines

Caco-2, a human colorectal adenocarcinoma cell line obtained from American Type Culture Collection (ATCC, Rockville, USA), was cultured in Dulbecco's Modified Eagle's medium (DMEM, Euroclone, Milan, Italy), supplemented with 20% fetal bovine serum (FBS), 1% L-glutamine and 1% Penicillin/Streptomycin (all Carlo Erba reagents, Milan, Italy) at 37 °C in 5% CO2.

2.9.2. MTS assay

Caco-2 cells were seeded in 96-well plates at a density of 5×10^3 cells/well in 100 µL of medium. After 24 h of incubation at 37 °C in 5% CO2, the cells were exposed to TQ-MP or TQ (1:200, 1:500 or 1:1000), for 2 h. Cell viability was assessed by a colorimetric method based on reduction of 3-(4,5-dimethylthiazol-2-yl)−5-(3-carboxymethoxyphenyl)−2-(4-sulfophenyl)−2H-tetrazolium, inner salt (MTS, Promega Corporation, Madison, USA). The optical density of the formazan product was measured at 490 nm using a VICTOR3 Wallac 1421 Multilabel Plate Reader (Perkin Elmer, Ramsey, USA). Data were expressed as percentage of viable cells compared to cells exposed to the solvent alone.

2.9.3. Transwell permeability studies

For transport studies, cells were seeded at 200,000 cells/well in cell, culture inserts with polyethylene terephthalate (PET) membranes (BRAND, Italy). Culture medium (DMEM) was added to apical (AP) and basolateral (BL) side and was replaced every day for the first week and daily, thereafter. Cells were let to differentiate for 18–21 days. The integrity of the layer was evaluated with the Lucifer Yellow (LY) permeability assay. LY was diluted in the transport buffer (Hank's Balanced Salt Solution, HBSS, with Ca2+, Mg2+, 25 mM HEPES, pH 7.4) and added to the AP compartment at a final concentration of 100 µM. After incubation at 37 °C for 1 h, the HBSS in the BL chamber was collected, and the concentration of LY determined by using 485 nm excitation and 530 nm emission, on a fluorescence plate reader (Multilabel Counter 1240 Victor 3, Perkin Elmer). The percentage of AP to BL permeability was calculated, according to the following equation:

% permeability = (Fluorescence in the BL-blank)/(Fluorescence LY-blank) *100

The critical maximum flux of LY to identify leaky monolayers was fixed to be less than 3% of starting concentration.

Transport studies were performed according to Hubatsch et al. (2007) and as previously reported (Piazzini et al., 2019), incubating TQ-MP or TQ (1:300) for 1 h in the apical compartment.

2.9.4. Up-take studies

To determine the ability to pass Caco-2 cellular membrane, cells were growth on glass cover-slips placed into 4-well plates for 24 h and then exposed to transport inhibitors (sodium azide 1 µM, chlorpromazine 15 µM, indomethacin 25 µM or verapamil 3 µM) for 30 min and then to FITC-MP 1:300, for 1 h, at 37 °C or maintained at 4 °C during the experiment. After that, cells were washed four times with PBS and fixed in 4% formaldehyde in 0.1 mol/L PBS pH 7.4, for 10 min at room temperature. After fixation, cells were washed four times with PBS and cell nuclei were stained with 40,6-diamidino-2-phenylindole (DAPI) for 10 min at room temperature. The cells were washed once with PBS and the cover-slips were glued to glass microscope slides and observed under a Olympus BX63 microscope equipped with a Metal Halide Lamp (Prior Scientific Instruments Ltd., Cambridge, United Kingdom) and a digital camera Olympus XM 10 (Olympus, Milan, Italy). Five photomicrographs were randomly taken for each sample and fluorescence was measured using ImageJ 1.33 image analysis software (http://rsb.info.nih.gov/ij, accessed on 12/3/21).

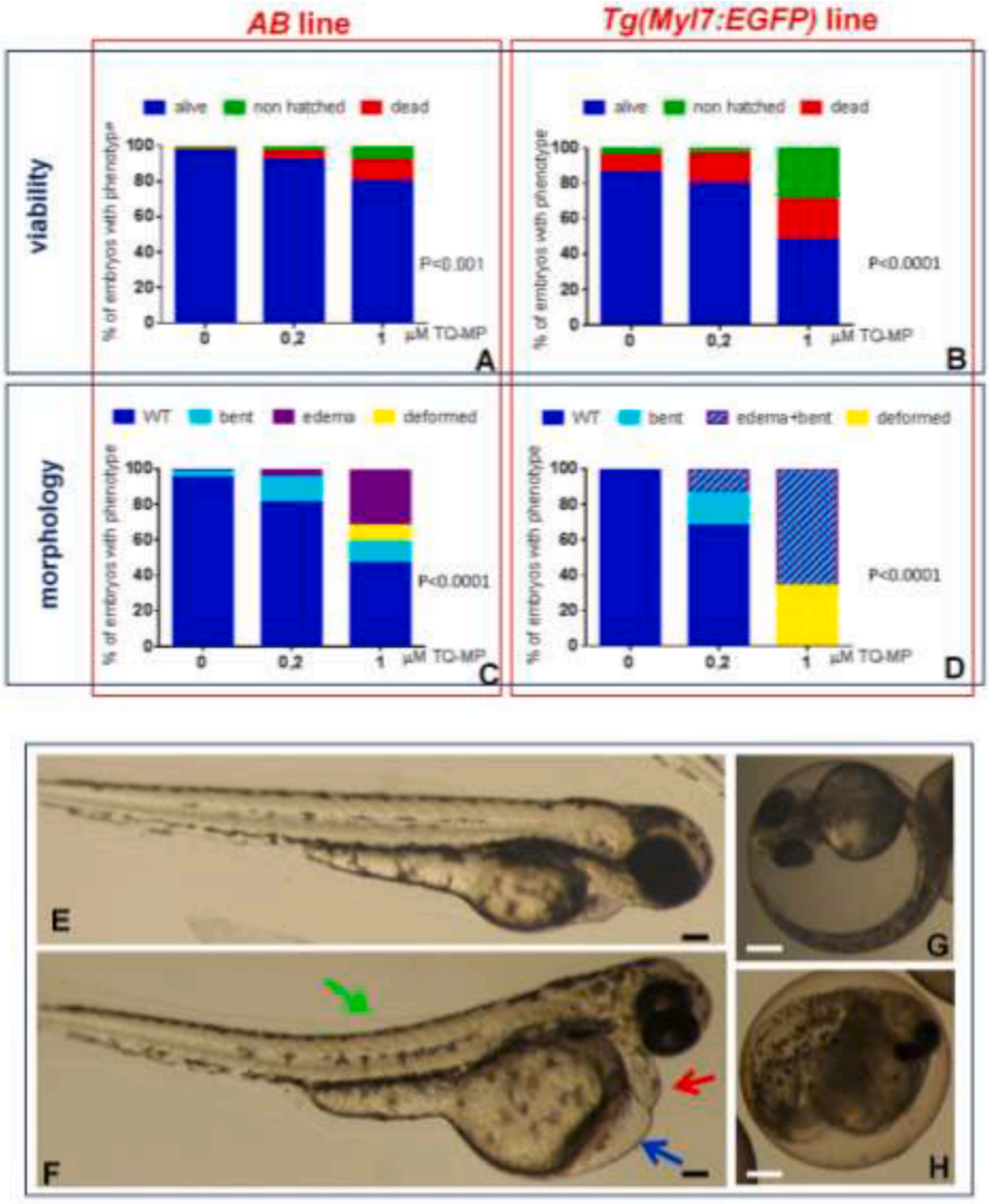

Fig. 10. Toxicity of TQ-MP in zebrafish embryos of *AB* and *Tg(Myl7:EGFP)* line. Analysis of *AB* (A,C) and *Tg(Myl7:EGFP)* (B,D) embryos developed in the presence of increasing concentrations of TQ-MP. The different analyses were performed at different moment of the development as described in materials and methods. In *Tg (Myl7:EGFP)* all the embryos with edema showed also axial-tail curvature. All values reported were the mean of 3 independent experiments. ≥ 30 embryos for each treated group were analyzed. Fisher's test analysis was performed on these data. E-H bright field images representative of unexposed (E,G) and 1 µM TQ-MP exposed 48hpf *AB* embryos. In F the embryo shows cardiac (red arrow) and ventral (blu arrow) edemas and axial-tail curvature (green arrow). In H a degenerated embryo still inside the chorion is shown. Scale bars 200 µm.

2.10. hCMEC/D3 cell culture experiments

2.10.1. hCMEC/D3 cell culture

This cell line (Millipore Cat. # SCC066) derives from human temporal lobe micro-vessels isolated from tissue excised during surgery for epilepsy control. Cells were seeded in a concentration of 2.5×10^4 cells/cm^2 and grown at 37 °C in an atmosphere of 5% CO2 in 25 cm^2 rat tail collagen type I coated culture flasks. EndoGROTM-MV Complete Media Kit (Cat. # SCME004) supplemented with 1 ng/mL FGF-2 (Cat. #GF003) was changed every three days and cells were grown until they were 90% confluent. Cells were passaged at least twice before use. Confluent hCMEC/D3 cells were split by AccumaxTM Cell Counting Solution in DPBS.

2.10.2. MTT assay

To assess cell viability after TQ and TQ-MP exposure, a 3-(4,5-Dimethylthiazol-2-yl)−2,5-diphenyltetrazolium bromide (MTT) assay was performed (Piazzini et al., 2020) Cells were seeded in a 24-well plate (6×10^4 cells/cm^2) pre-coated with Collagen Type I, Rat Tail (Cat. #08–115) and grown at 37 °C in an atmosphere of 5% CO2 in

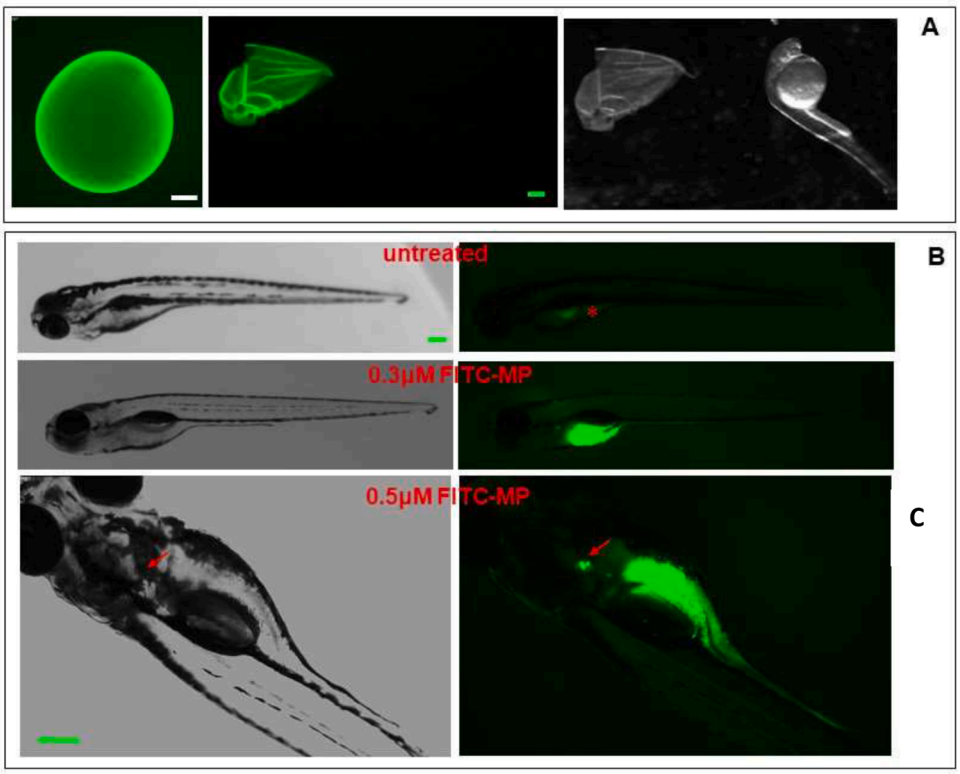

Fig. 11. FITC-MP biodistribution. *AB* embryos were exposed to 0.3 μM of FITC-MP. A: Nanomicelles stuck on the embryo chorion membrane: images of representative 24 hpf embryo still inside the chorion (left side) and after manual chorion removing in bright-field (right side) and in fluorescence (center). B: Images of representative 72 hpf embryos exposed (bottom) or not (top) to 0.3 μM of FITC-MP. Asterix in B indicates an autofluorescence signal of the embryo. C: 0.5 μM of FITC-MP were administered to 72 hpf embryos and analyzed 48 h later: besides the gastrointestinal tract, fluorescence was evident in the glomerulus (red arrows). White scale bar 200 μM, green scale bar 500 μM.

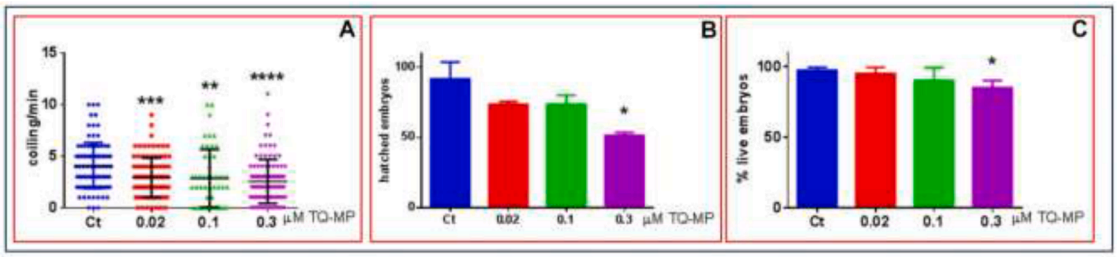

Fig. 12. Toxicity of TQ-MP on *Tg(Myl7:EGFP)* embryo development. (A) coiling test analysis was performed on 27 hpf embryos, hatched embryos (B) were counted at 53 hpf and the number of live embryos (C) was evaluated on embryos at 5 dpf. All values reported were the mean of 3 independent experiments. ≥ 30 embryos for each treated group were analyzed. *$P<0.05$, **$P<0.01$, ***$P<0.001$, ****$P< 0.0001$.

EndoGROTM Basal Medium (EBM-2). When the cells were approximately 70–80% confluent they were incubated with different concentrations of TQ and TQ-MP obtained by dilution (1: 100, 1: 300 and 1: 500) of a solution of TQ (5 mg / mL in DMSO) and of the formulation in EBM-2 for 2 and 4 h. The medium of each well was separated from the cells and stored for lactate dehydrogenase (LDH) assay, and cells were treated with 1 mg/mL of MTT for 30′ h at 37 °C and 5% CO2. Finally, DMSO was added to dissolve MTT formation and absorbance was measured at 550 and 690 nm. Cell viability was expressed as a percentage compared to the cells incubated only with EBM-2 (positive control). Triton X-100 was used as the negative control.

2.10.3. LDH assay

Cytotoxicity after TQ and polymeric micelles exposure was verified with LDH assay (Conti et al., 2010). The medium resulting from incubation of TQ and MP with cells was centrifuged (250 g, 10 min at RT) and the supernatant separated from the deposited cells in each well. This centrifugation process allowed us to remove any waste and cellular debris as well as TQ and TQ-MP. The release of LDH into culture supernatants was detected by adding catalyst and dye solutions of a Cytotoxicity Detection Kit (LDH) (Roche Diagnostics, Indianapolis, IN, USA). The absorbance values were recorded at 490 nm and 690 nm. Cytotoxicity was expressed as a percentage compared to the maximum LDH release in the presence of triton X-100 (positive control). EBM-2 was used as negative control since no cytotoxicity was detected in such conditions.

2.10.4. hCMEC/D3 cell permeability studies

For the permeation study of TQ and TQ-MP were used high density pore (2×10^6 pores/cm^2) transparent PET membrane filter inserts (0.4 μm, 23,1 mm diameter, Falcon, Corning BV, Amsterdam, Netherlands) in 6-well cell culture plates (Falcon, Corning, Amsterdam, Netherlands) for all transcytosis assays. The transparent PET membrane filter inserts were coated with rat tail collagen type I at a concentration of 0.1 mg/mL and incubated at 37 °C for 1 h prior to cell barrier coating. Inserts were subsequently washed with PBS and incubated for 1 h, after which PBS was removed and replaced with the assay medium. The inserts were calibrated for at least 1 h with assay medium at 37 °C. Optimum media volumes were calculated to be 1 mL and 1.2 mL respectively for apical and basolateral chambers (Piazzini et al., 2018). The transwell inserts were calibrated with assay medium for 1 h, then the medium was removed and hCMEC/D3 cells were seeded onto the apical side of the

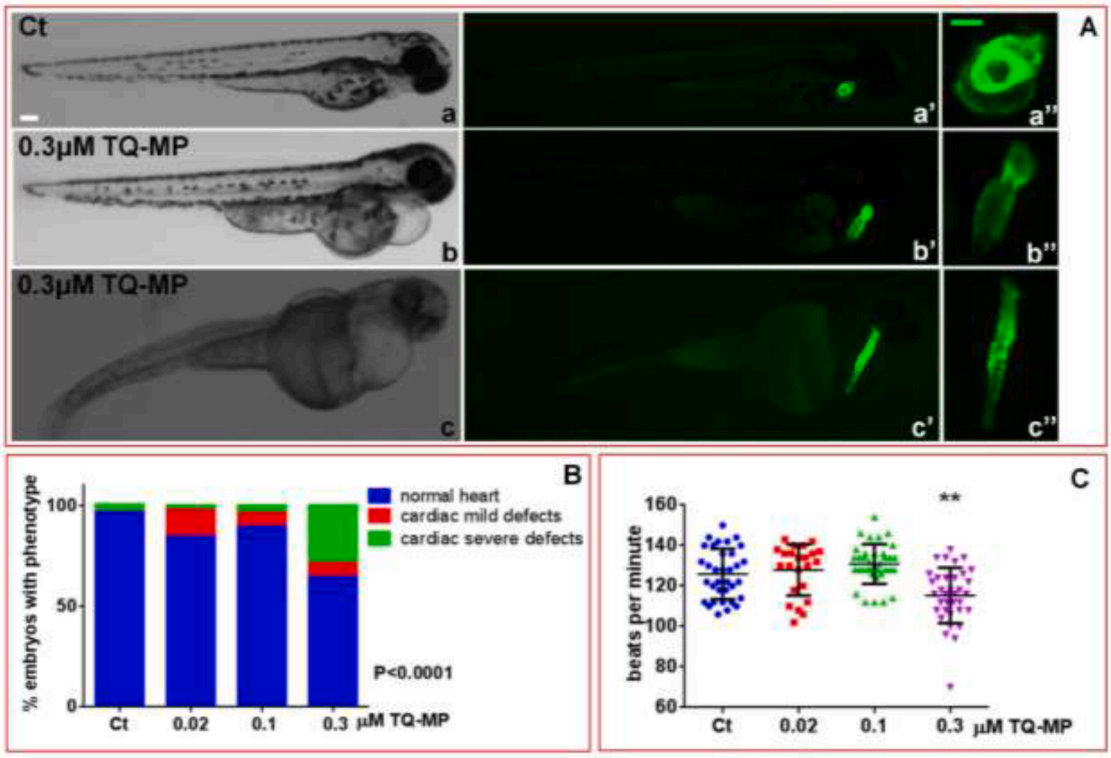

Fig. 13. Toxicity of TQ-MP on *Tg(Myl7:EGFP)* cardiac development. *Tg(Myl7:EGFP)* embryos were exposed to increasing amounts of TQ-MP. A: Images of representative 72 hpf *Tg(Myl7:EGFP)* embryo phenotypes. a-c bright field, a'-c' fluorescent images. a''-c'' magnification of the cardiac areas. B: Percentage of embryos with the indicated phenotypes, averaged across multiple independent experiments carried out in double blind. Fisher's test analysis was performed on these data. C: Quantification of heart beats/min in 72 hpf embryos. ** $P<0.01$. White scale bar 500 µm, green scale bar 200 µm.

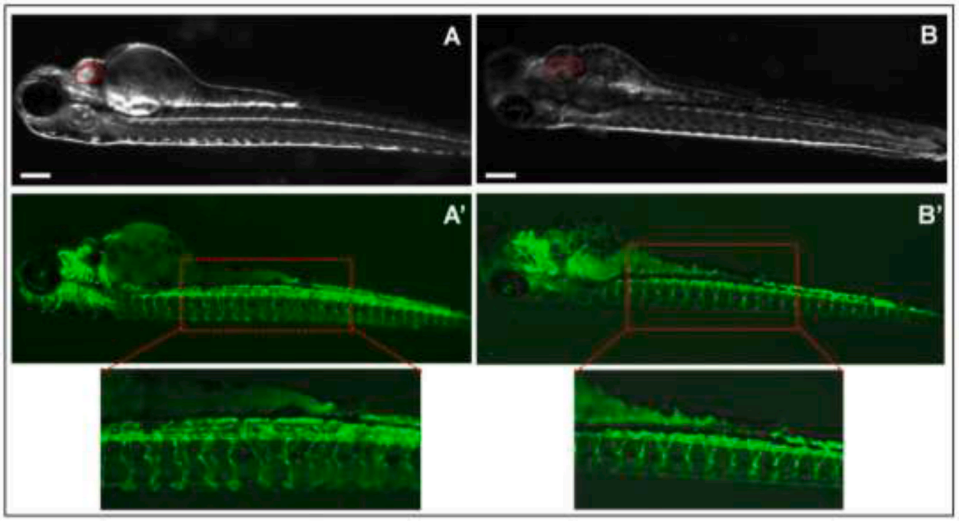

Fig. 14. Exposure to TQ-MP does not affect blood vessel development. Images of representative 72 hpf *Tg(Myl7:EGFP)* embryos exposed to 0.3 µM of TQ-MP. In A-A' an embryo with normal heart is shown while B,B' images present an embryo with no looping heart and cardiac edema. In A and B red dotted lines mark heart contours. Scale bar 500 µm.

inserts at a density of 6×10^4 cells/cm^2 in 1 mL assay media. 1.2 mL of fresh medium was added to the basolateral chamber. The assay medium was changed every 3 days following transwell apical insert seeding with hCMEC/D3. For seven days, cells were grown to confluence. hCMEC/D3 monolayers were used as a permeability assay for AG and AG-loaded liposomes. Fluorescein sodium salt (NaF) was considered at a concentration of 10 µg/mL as an integrity control marker with a known permeability coefficient (Papp) for this cell line (Piazzini et al., 2018; Gulyaev et al., 1999). For permeability studies, TQ (5 mg/mL) and TQ-MP (TQ 5 mg/mL) were diluted 1:500 in EBM-2 and added to the donor compartment, where they were left to incubate for 1 and 2 h. At the end of the incubation, the amount of NaF and TQ were quantified both in apical and basolateral compartments by HPLC-FLD or HPLC-DAD method. The apparent permeability coefficients (Papp) of free TQ and TQ loaded in MP were calculated according to the equation (Piazzini et al., 2018):

$$P_{app} = \frac{Vd}{A\ x\ Md}\ x\frac{Ma}{t}$$

where:

Papp: apparent permeability coefficient (cm/s); Vd: volume of the donor compartment (cm^3); A: area of membranes (cm^2); Md: donor amount (mol); Ma: apical amount (mol); t: incubation time (seconds).

2.11. Studies in vivo in zebrafish

2.11.1. Maintenance of zebrafish lines and breeding

The zebrafish facility has held the authorization n°297/2012-A since 12/21/2012. All animal procedures conform to the guidelines from Directive 2010/63/EU of the European Parliament regarding the protection of animals used for scientific purposes. Wild type AB, *Tg(myl7:EGFP)* and *Tg(flk1-GFP)* zebrafish lines were used in this study.

Zebrafish were raised in Tecniplast housing systems (Zebtec and Standalone systems) in 14 hrs light and 10 hrs dark at 28 °C. Zebrafish diet consisted of microgranular food (Sparos, Portugal) and Artemia salina (Artemia magnetica from INVE acquatica, INVE technologies, Belgium). Tricaine (3-amino benzoic acid ethylester) was purchased from Sigma (Cat.# A-5040) and used for embryo sedation.

2.11.2. Embryo toxicity study

Healthy zebrafish eggs were collected at 4 h post fertilization (hpf), washed in embryo medium and placed into 6-well culture plates at the density of 30–40 eggs/well. TQ-MP or FITC-MP at the indicated concentrations were added to the embryo water at 5hpf. Stereomicroscope (Leica M80) attached to a Nikon DS-Fi1 CCD camera was used to directly evaluate coiling movements (27hpf), possible presence of body malformations (72hpf), hatching rate (53hpf) and survival rate (5dpf). A fluorescence Leica DM IL microscope and a Nikon YFL microscope both equipped with CoolSnap CF camera (Photometric) were used to evaluate vessel development, cardiac morphology and heart beat rate at 72hpf. For heart beat analysis embryos were sedated by adding tricaine to the embryo water at the final concentration of 0.01 mg/ml. Videos (3 videos of 30 s each) were acquired from Selected Regions fixed on the fluorescent atrium and ventricle. In each video atrium and ventricle beats were simultaneously recorded. The heart rate was successively measured analysing the tracking signal obtained. All experiments were performed three times to maintain an accuracy statistic. NIS-Elements F 3.0 software was used to perform both bright and fluorescence imaging.

2.12. Statistical analysis

The experiments were repeated three times and results expressed as a mean ± standard deviation. Statistical significance of Caco-2 and hCMEC/D cells viability and cellular uptake was analyzed using one-way ANOVA followed by the post hoc Tukey's w-test for multiple comparisonsAll statistical calculations were performed using GRAPHPAD PRISM v. 8 for Windows (GraphPad Software, San Diego, CA, USA). A probability value $P < 0.05$ was considered significant. Statistical differences of Zebrafish toxicity study were determined by unpaired *t*-test, and Fisher's test with values of $P<0.05$ considered statistically significant.

3. Results and discussion

3.1. Characterization of TQ-MP

The optimized TQ-MP were prepared using Soluplus® (20 mg/mL), Solutol® (80 mg/mL) and TQ (5 mg/mL) (Bergonzi et al., 2020). Dynamic and Electrophoretic light scattering were used to characterize size, PdI and z-potential of the polymeric micelles (Table 1). The presence of TQ does not influence the stability of MP, when TQ were loaded into the micelles, the formulation showed the same physical parameters than empty MP. PdI < 0.2 and dimensions < 200 nm indicated respectively that the formulation was homogeneous and suitable for both oral and parenteral administration and it was able to load 5 mg/mL of TQ, increasing the aqueous solubility of TQ of 10 folds, with an EE% of 92.4 ± 0.3%. TEM micrographs provided information on morphology and dimensions of TQ-PM, the formulation had a spherical structure with a diameter close to that obtained through DLS analyses, 50–60 nm (Fig. 1).

FITC, a lipophilic fluorescent dye, was incorporated into MP as a probe to elucidate trans-epithelial transport *in vitro* studies with Caco-2 cells and to performed *in vivo* analyses in Zebrafish. The physical and chemical parameters of FITC-MP are shown in Table 1.

3.2. Stability of TQ-MP toward dilution

The TQ-MP were diluted with deionized water to evaluate the physical stability of the formulation. The system remains unchanged until the dilution of 1:300 v/v, beyond a little increase in size and PdI was observed. The EE% was unmodified (Table 2).

3.3. Stability in simulated gastrointestinal fluids

The stability of the formulation was also determined in simulated gastrointestinal conditions to verify if the polymeric micelles are able to protect TQ from degradation during gastrointestinal transit. To simulate this condition, TQ-MP was incubated at 37 °C in SGF in presence of pepsin followed by SIF in presence of the pancreatin-lipase-bile salts mixture. After 2 h of incubation in SGF micelles resulted physically and chemically stable and after 6 h of incubation in SIF, polymeric micelles resulted quite physically stable while the EE% was reduced, but still remains high, with a value of 62.9%.

3.4. In vitro release of TQ in simulated gastrointestinal fluids

The TQ release from MP was compared with the aqueous saturated solution (Fig. 2). In the gastric fluid during 2 h, only 8.2% of the TQ was released from MP and 9.2% was released in the intestinal environment within 6 h. Therefore, 82.6% of TQ remains encapsulated in MP, enhancing intestinal absorption. The lower release of TQ from MP and the physical and chemical stability in simulated gastro-intestinal conditions suggest that the formulation protects TQ from degradation and guarantees a slow release of TQ. Instead, free TQ follows an immediate release in SGF and SIF. The 16.7% of TQ was released from the aqueous saturated solution in the SGF after 2 h and the 20.7% in the SIF after 6 h. The same behavior was observed in PBS (pH = 7.4) (Bergonzi et al., 2020). Therefore, MP demonstrated promising potential to prevent burst release and the degradation of TQ after oral administration.

3.5. In vitro release of FITC

The FITC release in PBS was considered to evaluate the stability of dye loaded MP *in vitro* up-take studies in Caco-2 cells and *in vivo* studies in Zebrafish.

As demonstrated by Fig. 3, the release of FITC takes place gradually until a percentage of 12.8% after 24 h and it reaches the plateau, about 21%, at 48 h. This finding confirmed that FITC was stably delivered in the MP and it is not released from the MP during the *in vitro* and *in vivo* experiments.

Furthermore, as evidenced by the stability study at 4 °C for 10 days, the particle size, PdI, z-potential and EE% of the FITC-MP remained unchanged. In particular, sizes ranged from 43 ± 0 nm to 42 ± 1, nm, PdI from 0.18 ± 0.01 to 0.19 ± 0.01, z-potential from −8.9 ± 1.1 to −10.0 ± 1.1 and EE% from 85.3 ± 2.3 to 78.6 ± 1.7.

3.6. PAMPA studies

The PAMPA is an *in vitro* method used to evaluate the transcellular passive permeability. PAMPA could be a helpful complement to *in vitro* cells assays with Caco-2 and hCMEC/D3 to predict the oral and blood brain barrier absorption, respectively (Piazzini et al., 2019; Graverini et al., 2018, 2018; Navarro del Hierro et al., 2020). In PAMPA-gastric the effective permeability (Pe) value of TQ encapsulated in polymeric micelles was 12.0×10^{-5} cm/s after 1 hour and 7.7×10^{-5} cm/s after 2 h. Pe of free TQ was 3.0×10^{-5} cm/s after 1 hour and 4.5×10^{-5} cm/s after 2 h (Fig. 4). The results show that the use of MP significantly improves the permeation of TQ respect to saturated aqueous solution due to the presence of Solutol® and Soluplus® HS15, both solubilizing agents and Soluplus® penetration enhancer. The micelles increase of 10 times the TQ quantity in the donor compartment, improving the passive diffusion across the membrane.

The same trend was not observed in the PAMPA-brain experiments (Fig. 5). The free TQ has a Pe larger than the formulated TQ, 9.7×10^{-5} cm/s and 0.9×10^{-5} cm/s at 1 h, respectively and 12×10^{-5} cm/s and 3.1×10^{-5} cm/s at 2 h, respectively. This is probably due to the fact that TQ is a small molecule with a molecular weight of 164.20 g/mol and it has a good diffusivity through the lipid porcine brain membrane, while TQ-MP, despite having nanometric dimensions, slow down the passage, especially at shorter times. However, as reported in the case of PAMPA-gastric experiment, if we consider the quantity of TQ that crosses the membrane, it is much higher in the case of the TQ-MP respect to free TQ, 0.84 μg and 0.06 μg, respectively after 120 min. Then, the formulation ameliorates the permeation increasing the amount of substance that passes from the donor to the acceptor compartment.

3.7. Caco-2 cells permeability study

TQ alone or formulated in MP did not exhibited any cytotoxicity at concentration above 1:200, after 2 h of exposure (data not shown). As reported in Fig. 6A, TQ-MP had a higher apparent permeability (P_{app}) compared with TQ alone in AP-BL experiments: specifically, at 30 min TQ was not detected into the basolateral chamber and exhibited a lower permeability after 1 hour of incubation compared to TQ-MP. Considering the amount of substance permeated, the behavior was the same (Fig. 6B), with 9.2 ng and 6.5 ng permeated from TQ-MP and TQ solution, respectively, confirming the findings obtained with PAMPA test. The nanoformulation has a positive effect also on the active permeation of TQ.

The mechanisms involved in the internalization of micelles were further explored performing uptake experiments with FITC-MP in the presence of an energy depletion agent (sodium azide), a clathrin-dependent endocytosis inhibitor (chlorpromazine), a caveolin-dependent endocytosis inhibitor (indomethacin), a P-gp inhibitor (verapamil) or setting the temperature at 4 °C to inhibit active uptake processes. As can be seen in the graphic 7 G, the transport of the micelles is temperature-dependent and it is statistically reduced in the presence of verapamile suggesting the involvement of ABC-binding cassette transporters in their internalization. The reduction, although not statistically significant in the presence of sodium azide and indomethacin, however suggests the presence of endocytosis and ATP-dependent mechanisms (as in the case of Pgp).

The decrease of cellular uptake in the presence of inhibitors and at low temperature, pointed out by the reduced intracellular FITC, green signal intensity, suggested that the Caco-2 cell monolayers actively take up FITC-MP by endocytosis and that P-gp efflux pump are also involved (Fig. 7A-F).

3.8. MTT and LDH assays

The human endothelial cell line hCMEC/D_3 of the cerebral microcirculation was used as a model of the human BBB to predict the P_{app} of free and formulated TQ. In fact, these cells express many of the transporters and receptors of the human BBB. MTT and LDH tests were performed in the hCMEC/D3 cell line to evaluate the effect of TQ and TQ-MP. When we exposed the cells to different concentrations of TQ and TQ-MP for 2 h (Fig. 8A), no significant changes in MTT were observed, with the exception of sample diluted 1:100, or LDH release compared to cells exposed to EBM-2 medium alone, indicating that TQ and TQ-MP modify neither the metabolic activity of the cells nor the integrity of the membrane at these time points.

When the cells were incubated for 4 h with TQ no toxicity was observed, while the TQ-MP diluted 1:100 and 1:300 induced a significant reduction in cell viability and an increase in cytotoxicity compared to the control (Fig. 8B). From these results we have chosen a dilution of 1:500 and a time point of 2 h to performed the permeation experiments.

3.9. BBB permeability studies

We performed permeability studies to predicted the ability of TQ and TQ-MP to across the blood brain barrier using hCMEC/D3 cells apparent permeability coefficient (P_{app}) that correlates with *in vivo* permeability data. NaF was used as the negative control and its P_{app} was determined during all transport experiments to monitor the integrity of the cell layer. The hCMEC/D3 cells were incubated with pure TQ and TQ-MP both diluted 1:500, for 2 h. Then samples were taken in the donor and acceptor compartment 1 and 2 h after the treatment. To check the integrity of the layer, the NAF probe was also quantified in each sample. The NAF Papp was $8.41 \pm 1 \times 10^{-6}$ cm/s, in agreement with the literature value (Graverini et al., 2018; Piazzini et al., 2018). This value remained constant during all the experiments, demonstrating the integrity of the confluence of the layer and the tight junctions. P_{app} values of TQ-MP after 1 h and 2 h were more high of the free drug TQ. These results show that the polymeric micelles are able to enhance the permeability of TQ trough the BBB (Fig. 9A). The different result obtained with the cells compared to the PAMPA test suggests that probably active mechanisms are involved in the passage of the TQ-MP.

As show in Fig. 9B the amount of TQ permeated across hCMEC/D3 cells layer was significantly increase with the nanoformulation both 1 and 2 h even in the case of the cell test.

3.10. In vivo toxicological studies in Zebrafish

Two different zebrafish lines were initially considered, the wild type (*AB*) line and the transgenic line *Tg(Myl7:EGFP)* in which cardiomyocytes are marked with green fluorescence protein (Huang et al., 2003) (Fig. 10). At the dose of 0.2 μM, referred to the quantity of TQ, the TQ-MP are little toxic in both lines with a marked reduction of dead, edema and the disappearance of deformations which instead are observed in the case of TQ-MP at the dose of 1 μM. At this dose the formulation strongly impacts embryo viability and morphology of both lines although the transgenic line showed a higher sensitivity. A significant decrease of hatching rate was observed in both lines after 1 μM TQ-MP exposure (Fig. 10A,B) while treated embryos showed a dose-dependent increase of axial-tail curvature and of cardiac edemas (Fig. 10C—H).

To be able to track micelles localization during the first days of zebrafish *AB* embryo development, we used FITC labeled micelles (FITC-MP). Although the diameter of the micelles is considerably smaller than that of the chorion pores (40–50 nm *versus* 0.5–0.7 μm of the chorion pores), FITC-MP appear to be not able to pass through the chorion membrane (Fig. 11A), as reflected by the absence of FITC signals inside embryos, as previously observed in the literature for PEG-b-PCL copolymeric nano-micelles (Zhou et al., 2016). Micelles stuck on the external surface of the chorion probably altering the passive diffusion of molecules trough this membrane. This effect might be responsible of the morphological and behavioral changes observed in embryos still inside the chorion exposed to TQ-MP (Fig. 10). 4dpf embryos developed in the

presence of FITC-MP show a strong fluorescent signal almost exclusively at the level of the gastrointestinal tract (Fig. 11B). At higher dosage (0,5 μM, freshly added to 72 hpf embryos to avoid high impact on development), the presence of polymeric micelles is also evident in the glomerulus (Fig. 11C).

The spontaneously occurring lateral tail coils generated from a single neural circuit is considered a valid test for detection of developmental neurotoxicity (Ogungbemi et al., 2020; Zindler et al., 2019). We exposed embryos to increasing doses of TQ-MP in the coiling test. TQ-MP at the dose of 1 μM induces severe alterations in all *Tg(Myl7:EGFP)* treated embryos (Fig. 10C—H), for this region lower doses were tested (0.02–0.3 μM range). At 27 hpf the coiling frequency resulted slightly but significantly reduced in all the treated embryos compared to the untreated ones (Fig. 12A) while only the embryos exposed to the 0.3 μM concentration showed a significant reduction of embryo hatching at 53 hpf (Fig. 12B) and viability at 96 hpf (Fig. 12C).

The more sensitive *Tg(Myl7:EGFP)* line which allows to analyze cardiac development and function by *in vivo* cardiac imaging was also applied to deeper investigate the TQ-MP toxicity on cardiac development. A dose-dependent increase of frequency and severity of cardiac defects was observed in embryos exposed to micelles in comparison with untreated embryos. Doses in the range 0.02–0.3 μM were tested.

TQ-MP 0.02 and 0.1 μM have small influence on both the morphology and the heartbeat, while the TQ-MP 0.3 μM affected also the cardiac functionality, significantly decreasing the heart rate (Fig. 13B,C). Embryos showing looping defects were indicated as mild cardiac phenotype while alterations of the heart chamber shape and heartstring like phenotype were classified as severe defects (Fig. 13A,B).

Cardiovascular problems and risk for cardiovascular disease-related events caused by micro/nanoparticles exposure were reported in the literature. Poly(ethylene glycol) (PEG)-b-poly(ε-caprolactone) nanoparticles caused embryo mortality and malformations in a dose dependent manner (Zhou et al., 2016). The exposure to different engineered nanoparticles poses risks to cardiovascular problems (Duan et al., 2013; Chen et al., 2015).

Then, we verified whether the TQ-loaded Soluplus®-Solutol® HS15 micelles might affect also blood vessel development exploiting the *Tg (flk1-GFP)* line which expresses GFP under the control of the vascular endothelial growth factor receptor 2 (vegfr2) promoter. As evident in Fig. 14B,B' even embryos whose cardiac development had been affected by TQ-MP 0.3 μM exposure did not show significant alteration of vessel morphology.

4. Conclusion

In summary, we demonstrated the significant increase of solubility and permeability of TQ due to its formulation in Soluplus®-Solutol® HS15 polymeric micelles, as demonstrated by PAMPA experiments, in particular in the case of PAMPA-gastric test. TQ-MP had a higher apparent permeability compared with TQ alone in both Caco-2 and hCMEC/D3 cells. The decrease of cellular uptake in the presence of inhibitors and at low temperature suggested that the Caco-2 cell monolayers actively take up MP by endocytosis and that P-gp efflux pump are also involved. The analysis of different endpoints in Zebrafish demonstrates that TQ-MP do not induce toxic effects at concentrations below 0.3 μM in both lines wild type (*AB*) and the transgenic *Tg(Myl7:EGFP)*. At the dose of 0.2 μM there is a marked reduction of dead, edema and the disappearance of deformations compared to 0.3 μM trated embryos. TQ-MP between 0.02 and 0.1 μM have small influence on both the morphology and the heartbeat, while the TQ-MP 0.3 μM affect also the cardiac functionality, significantly decreasing the heart rate, but it does not show significant alteration of vessel morphology. Then the polymeric micelles represent an effective carrier to improve the biopharmaceutical properties of TQ and zebrafish is a useful model for *in vivo* toxicological study of nanomedicines.

CRediT authorship contribution statement

Jessika Lodovichi: Methodology, Validation, Investigation, Data curation, Writing – original draft. **Elisa Landucci:** Conceptualization, Methodology, Validation, Investigation, Resources, Data curation, Writing – original draft, Writing – review & editing. **Letizia Pitto:** Conceptualization, Methodology, Resources, Data curation, Writing – original draft, Writing – review & editing. **Ilaria Gisone:** Validation, Investigation. **Mario D'Ambrosio:** Methodology, Validation, Investigation, Data curation, Writing – original draft. **Cristina Luceri:** Conceptualization, Resources, Data curation, Writing – original draft, Writing – review & editing, Supervision. **Maria Cristina Salvatici:** Methodology. **Maria Camilla Bergonzi:** Conceptualization, Methodology, Resources, Writing – original draft, Writing – review & editing.

Acknowledgments

The authors thank MIUR-Italy ("Progetto dipartimenti di eccellenza 2018–2022" allocated to the Department of Chemistry "Ugo Schiff", University of Florence, Italy).

References

Azhari, H., Younus, M., Hook, S.M., Boyd, B.J., Rizwan, S.B., 2021. Cubosomes enhance drug permeability across the blood–brain barrier in zebrafish. Int. J. Pharm. 600, 120411.

Ballout, F., Habli, Z., Rahal, O.N., Fatfat, M., Gali-Muhtasib, H., 2018. Thymoquinone-based nanotechnology for cancer therapy: promises and challenges. Drug Discov. Today 23, 1089–1098.

Banerjee, S., Padhye, S., Azmi, A., Wang, Z.W., Philip, P.A., Kucuk, O., Sarkar, F.H., Mohammad, R.M., 2010. Review on molecular and therapeutic potential of thymoquinone in cancer. Nutr. Cancer 62, 938–946.

Bergonzi, M.C., Hamdouch, R., Mazzacuva, F., Isacchi, B., Bilia, A.R., 2014. Optimization, characterization and *in vitro* evaluation of curcumin microemulsions. LWT-Food Sci. Technol. 59, 148–155.

Bergonzi, M.C., Vasarri, M., Marroncini, G., Barletta, E., Degl'Innocenti, D., 2020. Thymoquinone-Loaded Soluplus®-Solutol® HS15 Mixed Micelles: preparation, In Vitro Characterization, and Effect on the SH-SY5Y Cell Migration. Molecules 25 (20), 4707.

Bhattacharjee, S., 2016. DLS and zeta potential – What they are and what they are not? J. Control. Release 235, 337–351.

Bilia, A.R., Piazzini, V., Risaliti, L., Vanti, G., Casamonti, M., Wang, M., Bergonzi, M.C., 2018. Nanocarriers: a successful tool to increase solubility, stability and optimise bioefficacy of natural constituents. Curr. Med. Chem. 25, 1–24.

Calienni, M.N., Cagel, M., Montanari, J., Moretton, M.A., Prieto, M.J., Chiappetta, D.A., Del Valle Alonso, S., 2018. Zebrafish (Danio rerio) model as an early stage screening tool to study the biodistribution and toxicity profile of doxorubicin-loaded mixed micelles. Toxicol. Appl. Pharmacol. 357, 106–114.

Cassano, D., Mapanao, A., Summa, M., Vlamidis, Y., Giannone, G., Santi, S., Guzzolino, E., Pitto, L., Poliseno, L., Bertorelli, R., Voliani, V., 2019. Biosafety and biokinetics of noble metals: the impact of their chemical nature. ACS Appl. Bio Mater. 2, 4464–4470.

Chakraborty, C., Hsu, C.H., Wen, Z.H., Lin, C.S., Agoramoorthy, G., 2009. Zebrafish: a complete animal model for *in vivo* drug discovery and development. Curr. Drug Metab. 10, 116–124.

Chen, Z., Wang, Y., Zhuo, L., et al., 2015. Effect of titanium dioxide nanoparticles on the cardiovascular system after oral administration. Toxicol Lett 239, 123–130.

Conti, P., Pinto, A., Tamborini, L., Madsen, U., Nielsen, B., Bräuner-Osborne, H., Hansen, K.B., Landucci, E., Pellegrini-Giampietro, D.E., De Sarro, G., Donato Di Paola, E., De Micheli, C., 2010. Novel 3-carboxy- and 3-phosphonopyrazoline amino acids as potent and selective NMDA receptor antagonists: design, synthesis, and pharmacological characterization. ChemMedChem 5, 1465–1475.

CTRI / 2020 /05/025167. http://ctri.nic.in/Clinicaltrials/showallp.php?mid1=43378&EncHid=&userName=thymoquinone.

D'Amora, M., Cassano, D., Pocoví-Martínez, S., Giordani, S., Voliani, V., 2018. Biodistribution and biocompatibility of passion fruit-like nano-architectures in zebrafish. Nanotoxicol 12, 914–922.

Darakhshan, S., Pour, A.B., Colagar, A.H., Sisakhtnezhad, S., 2015. Thymoquinone and its therapeutic potentials. Pharmacol. Res. 95-96, 138–158.

Di, L., Kerns, E.H., Fan, K., McConnell, O.J., Carter, G.T., 2003. High throughput artificial membrane permeability assay for blood–brain barrier. Eur. J. Med. Chem. 38, 223–232.

Duan, J., Yu, Y., Li, Y., Sun, Z., 2013. Cardiovascular toxicity evaluation of silica nanoparticles in endothelial cells and zebrafish model. Biomaterials 34, 5853–5862.

El-Far, A.H., Al Jaouni, S.K., Li, W., Mousa, S.A., 2018. Protective Roles of Thymoquinone Nanoformulations: potential Nanonutraceuticals in Human Diseases. Nutrients 10, 1369.

El-Far, A.H., Tantawy, M.A., Al Jaouni, S.K., Mousa, S.A., 2020. Thymoquinone-chemotherapeutic combinations: new regimen to combat cancer and cancer stem cells. Naunyn Schmiedebergs Arch. Pharmacol. 393, 1581–1598.
Fako, V.E., Furgeson, D.Y., 2009. Zebrafish as a correlative and predictive model for assessing biomaterial nanotoxicity. Adv. Drug Deliv. Rev. 61, 478–486.
Farkhondeh, T., Samarghandian, S., Borji, A., 2017. An overview on cardioprotective and antidiabetic effects of thymoquinone. Asian Pac. J. Trop. Med. 10, 849–854.
Graverini, G., Piazzini, V., Landucci, E., Casamenti, F., Pantano, D., Pellegrini-Giampietro, D., Bilia, A.R., Bergonzi, M.C., 2018. Solid lipid nanoparticles for delivery of andrographolide across the blood-brain barrier: *in vitro* and *in vivo* evaluation. Colloid. Surf. B Biointerfaces 161, 302–313.
Gulyaev, A.E., Gelperina, S.E., Skidan, I.N., Antropov, A.S., Kivman, G.Y., Kreuter, J., 1999. Significant transport of doxorubicin into the brain with polysorbate 80-coated nanoparticles. Pharm. Res. 16, 1564–1569.
Haque, E., Ward, A.C., 2018. Zebrafish as a model to evaluate nanoparticle toxicity. Nanomaterials 8, 561.
Hou, J., Suna, E., Sunb, C., Wanga, J., Yanga, L., Jiaa, X., Zhang, Z., 2016. Improved oral bioavailability and anticancer efficacy on breast cancer of paclitaxel via Novel Soluplus-Solutol HS15 binary mixed micelles system. Int. J. Pharm. 512, 186–193.
Huang, C.J., Tu, C.T., Hsiao, C.D., Hsieh, F.J., Tsai, H.J., 2003. Germ-line transmission of a myocardium-specific GFP transgene reveals critical regulatory elements in the cardiac myosin light chain 2 promoter of zebrafish. Dev. Dyn. 228, 30–40.
Hubatsch, I., Ragnarsson, E.G., Artursson, P., 2007. Determination of drug permeability and prediction of drug absorption in Caco-2 monolayers. Nat. Protoc. 2, 2111–2119.
Jia, H.R., Zhu, Y.X., Duan, Q.Y., Chen, Z., Wu, F.G., 2019. Nanomaterials meet zebrafish: toxicity evaluation and drug delivery applications. J Control Release 311-312, 301–318.
Kalaiarasi, S., Arjun, P., Nandhagopal, S., Brijitta, J., Iniyan, A.M., Vincent, S.G.P., Kannan, R.R., 2016. Development of biocompatible nanogel for sustained drug release by overcoming the blood brain barrier in zebrafish model. J. Appl. Biomed. 14, 157–169.
Kansy, M., Senner, F., Gubernator, K., 1998. Physicochemical high throughput screening: parallel artificial membrane permeation assay in the description of passive absorption processes. J. Med. Chem. 41, 1007–1010.
Kausar, H., Mujeeb, M., Ahad, A., Moolakkadath, T., Aqil, M., Ahmad, A., Akhter, H., 2019. Optimization of ethosomes for topical thymoquinone delivery for the treatment of skin acne. J. Drug Deliv. Sci. Technol. 49, 177–187.
Landucci, E., Mazzantini, C., Buonvicino, D., Pellegrini-Giampietro, D.E., Bergonzi, M.C., 2021. Neuroprotective effects of thymoquinone by the modulation of ER stress and apoptotic pathway in *in vitro* model of excitotoxicity. Molecules 26, 1592.
Li, Y., Song, X., Yi, X., Wang, R., Lee, S.M.-Y., Wang, X., Zheng, Y., 2017a. Zebrafish: a visual model to evaluate the biofate of transferrin receptor-targeted 7peptide-decorated coumarin 6 Micelles. ACS Appl. Mater. Interfaces 9, 39048–39058.
Li, Y., Chen, T., Miao, X., Yi, X., Wang, X., Zhao, H., Zheng, Y., 2017b. Zebrafish: a promising *in vivo* model for assessing the delivery of natural products, fluorescence dyes and drugs across the blood-brain barrier. Pharmacol. Res. 125, 246–257.
Li, Y., Miao, X., Chen, T., Yi, X., Wang, R., Zhao, H., Zheng, Y., 2017c. Zebrafish as a visual and dynamic model to study the transport of nanosized drug delivery systems across the biological barriers. Colloids Surf. B Biointerfaces 156, 227–235.
MacRae, C.A., Peterson, R.T., 2015. Zebrafish as tools for drug discovery. Nat. Rev. Drug Discov. 14, 721–731.
Malik, S., Singh, A., Negi, P., Kapoor, V.K., 2021. Thymoquinone: a small molecule from nature with high therapeutic potential. Drug Discov. Today. https://doi.org/10.1016/j.drudis.2021.07.013 in press.
Mostafa, M., Alaaeldin, E., Aly, U.F., Sarhan, H.A., 2018. Optimization and characterization of thymoquinone-loaded liposomes with enhanced topical anti-inflammatory activity. AAPS PharmSciTech 19, 3490–3500.
Navarro del Hierro, J., Piazzini, V., Reglero, G.J., Martin, D., Bergonzi, M.C., 2020. *In vitro* permeability of saponins and sapogenins from seed extracts by the parallel artificial membrane permeability assay (PAMPA): effect of *in vitro* gastrointestinal digestion. J. Agric. Food Chem. 68, 1297–1305.
Ogungbemi, A.O., Teixido, E., Massei, R., Scholz, S., Kuster, E., 2020. Optimization of the spontaneous tail coiling test for fast assessment of neurotoxic effects in the zebrafish embryo using an automated workflow in KNIME®. Neurotoxicol. Teratol. 81, 106918.
Pal, R.R., Rajpal, V., Singh, P., Saraf, S.A., 2021. Recent findings on thymoquinone and its applications as a nanocarrier for the treatment of cancer and rheumatoid arthritis. Pharmaceutics 13, 775.
Piazzini, V., D'Ambrosio, M., Luceri, C., Cinci, L., Landucci, E., Bilia, A.R., Bergonzi, M. C., 2019. Formulation of nanomicelles to improve the solubility and the oral absorption of silymarin. Molecules 24, 1688.
Piazzini, V., Landucci, E., Graverini, G., Pellegrini-Giampietro, D.E., Bilia, A.R., Bergonzi, M.C., 2018. Stealth and cationic nanoliposomes as drug delivery systems to increase andrographolide BBB permeability. Pharmaceutics 10, 128.
Piazzini, V., Landucci, E., Urru, M., Chiarugi, A., Pellegrini-Giampietro, D.E., Bilia, A.R., Bergonzi, M.C., 2020. Enhanced dissolution, permeation and oral bioavailability of aripiprazole mixed micelles: *in vitro* and *in vivo* evaluation. Int. J. Pharm. 583, 119361.
Pop, R.M., Sabin, O., Suciu, S., Vesa, S.C., Socaci, S.A., Chedea, V.S., Bocsan, I.C., Buzoianu, A.D., 2020. Nigella Sativa's anti-inflammatory and antioxidative effects in experimental inflammation. Antioxidants 9, 921.
Rabanel, J.M., Piec, P.A., Landri, S., Patten, S.A., Ramassamy, C., 2020. Transport of PEGylated-PLA nanoparticles across a blood brain barrier model, entry into neuronal cells and *in vivo* brain bioavailability. J. Control. Release 328, 679–695.
Rathore, C., Rathbone, M.J., Chellappan, D.K., Tambuwala, M.M., Pinto, T.D.J.A., Dureja, H., et al., 2020. Nanocarriers: more than tour de force for thymoquinone. Expert Opin. Drug Deliv. 17, 479–494.
Rathore, C., Upadhyay, N.K., Sharma, A., Lal, U.R., Raza, K., Negi, P., 2019. Phospholipid nanoformulation of thymoquinone with enhanced bioavailability: development, characterization and anti-inflammatory activity. J. Drug Deliv. Sci. Technol. 52, 316–324.
Salmani, J.M.M., Asghar, S., Lv, H., Zhou, J., 2014. Aqueous solubility and degradation kinetics of the phytochemical anticancer thymoquinone; probing the effects of solvents, pH and Light. Molecules 19, 5925–5939.
Sieber, S., Grossen, P., Bussmann, J., Campbell, F., Kros, A., Witzigmann, D., Huwyler, J., 2019. Zebrafish as a preclinical *in vivo* screening model for nanomedicines. Adv. Drug Deliv. Rev. 151-152, 152–168.
Tao, J., Wei, Z., He, Y., Yan, X., Ming-Yuen Lee, S., Wang, X., Ge, W., Zheng, Y., 2020. Toward understanding the prolonged circulation and elimination mechanism of crosslinked polymeric micelles in zebrafish model. Biomaterials 256, 120180.
Van Pomeren, M., Brun, N.R., Peijnenburg, W.J.G.M., Vijver, M.G., 2017. Exploring uptake and biodistribution of polystyrene (nano)particles in zebrafish embryos at different developmental stages. Aquatic Toxicol 190, 40–45.
Weber, G.E.B., Dal Bosco, L., Gonçalves, C.O.F., Santos, A.P., Fantini, C., Furtado, C.A., Parfitt, G.M., Peixoto, C., Romano, L.A., Vaz, B.S., Barros, D.M., 2014. Biodistribution and toxicological study of PEGylated single-wall carbon nanotubes in the zebrafish (Danio rerio) nervous system. Toxicol. Appl. Pharmacol. 280, 484–492.
Wu, Z., Koh, B., Lawrence, L.M., Kanamala, M., Pool, B., Svirskis, D., Dalbeth, N., Astin, J.W., Crosier, K.E., Crosier, P.S., Hall, C.J., 2019. Liposome-mediated drug delivery in larval zebrafish to manipulate macrophage function. Zebrafish 16, 171–181.
Zhou, T., Dong, Q., Shen, Y., Wu, W., Wu, H., Luo, X., Liao, X., Wang, G., 2016. PEG-b-PCL polymeric nano-micelle inhibits vascular angiogenesis by activating p53-dependent apoptosis in zebrafish. Int. J. Nanomed. 11, 6517–6531.
Zindler, F., Beedgen, F., Brandt, D., Steiner, M., Stengel, D., Baumann, L., Braunbeck, T., 2019. Analysis of tail coiling activity of zebrafish (Danio rerio) embryos allows for the differentiation of neurotoxicants with different modes of action. Ecotoxicol. Environ. Saf. 186, 109754.